Hemispheric asymmetries in cortical gray matter microstructure identified by neurite orientation dispersion and density imaging

Judith Schmitz [a,*], Christoph Fraenz [a], Caroline Schlüter [a], Patrick Friedrich [a], Rex E. Jung [b], Onur Güntürkün [a], Erhan Genç [a,1], Sebastian Ocklenburg [a,1]

[a] Biopsychology, Institute of Cognitive Neuroscience, Department of Psychology, Ruhr University, Bochum, Germany
[b] Department of Neurosurgery, University of New Mexico, Albuquerque, USA

ARTICLE INFO

ABSTRACT

Histological studies have reported microstructural hemispheric asymmetries in several cortical areas of the human brain, but reliable *in vivo* assessment methods have been lacking so far. Here, we used neurite orientation dispersion and density imaging (NODDI) to examine microstructural asymmetries in *in vivo* and determine if findings are in accordance with what has been reported in histological studies. We examined intra-neurite volume fraction (INVF), neurite orientation dispersion (ODI), and isotropic volume fraction (ISO) asymmetries in two independent samples of healthy adults (n = 269 and n = 251). Over both samples, we found greater left-hemispheric INVF in early auditory, inferior parietal and temporal-parietal-occipital areas. In contrast, we found greater right-hemispheric INVF in the fusiform and inferior temporal gyrus, reflecting what has been reported in histological studies. ODI was asymmetric towards the left hemisphere in frontal areas and towards the right hemisphere in early auditory areas. ISO showed less pronounced asymmetries. There were hardly any effects of sex or handedness on microstructural asymmetry as determined by NODDI. Taken together, these findings suggest substantial microstructural asymmetries in gray matter, making NODDI a promising marker for future genetic and behavioral studies on laterality.

1. Introduction

The left and right hemispheres of the human brain differ in several functional aspects, the most popular being handedness and language lateralization (Güntürkün and Ocklenburg, 2017; Ocklenburg and Güntürkün, 2018). However, the ontogenetic determinants of functional hemispheric asymmetries remain rather unclear (Armour et al., 2014; Brandler et al., 2013; Ocklenburg et al., 2014; Schmitz et al., 2017). In addition to gray matter asymmetries (Ocklenburg et al., 2016b), the structure of inter- and intrahemispheric white matter pathways have been proposed to contribute to functional hemispheric asymmetries (Ocklenburg et al., 2016a). On the microstructural level, neurites, i.e. dendrites and axons, constitute the "building blocks of the computational circuitry of the brain" (Zhang et al., 2012). Neurite orientation dispersion and density imaging (NODDI) is a diffusion MRI technique for *in vivo* quantification of neurite morphology in humans (Zhang et al., 2012). Specifically, it allows for the estimation of neurite density (intra-neurite

volume fraction, INVF), neurite orientation dispersion (ODI), a neurite tortuosity measure, and isotropic volume fraction (ISO). So far, no study has investigated hemispheric asymmetries in microstructure *in vivo*. However, the detection of microstructural asymmetry is an interesting marker not only for genetic and behavioral studies on hemispheric asymmetries, but also in the context of neurodevelopmental and psychiatric traits. Atypical microstructural asymmetry has been reported in schizophrenia patients (Chance, 2014; Chance et al., 2008; Cullen et al., 2006; Simper et al., 2011) and altered microstructure in autism spectrum disorder (Casanova et al., 2006; van Kooten et al., 2008) has been suggested to underlie atypical functional hemispheric asymmetries (Chance, 2014). In order to provide a reference for potential clinical studies, microstructural asymmetries in healthy subjects have to be established. Thus, the aim of the present study was the first whole brain investigation of gray matter microstructure by applying NODDI to two independent datasets constituting an overall sample of 520 healthy adults.

Several *post mortem* studies have reported hemispheric asymmetries

in microstructure (Schenker et al., 2009) with focus on different brain areas and different markers for microcircuitry (for a comprehensive overview see Table 1). The analysis of cell density has been proposed as an indirect way to estimate the amount of neuropil, i.e. dendrites, axons and synapses. For example, the gray-level index (GLI) estimates the fraction of tissue volume that is occupied by Nissl-stained cell bodies with decreased cell density indicating an increased proportion of neuropil (Amunts et al., 1996). A common feature of mammalian cytoarchitecture is the columnar organization of neurons surrounded by neuropil across cortical layers VI to II. Single vertical rows of neurons with a width of about 60–90 μm are known as minicolumns. Macrocolumns are constituted of several minicolumns, forming thalamocortical or corticocortical columns with a width of about 600–800 μm (Hutsler and Galuske, 2003). Seldon (1981a) suggested greater distance between minicolumns to reflect a higher amount of neuropil. Few studies have investigated hemispheric asymmetries in dendritic branching directly using Golgi impregnations (Seldon, 1982).

Previous histological studies report greater right-hemispheric neuron density in the *planum temporale* (parts of BA 22, BA 41, and BA 42) (Buxhoeveden et al., 2001; Smiley et al., 2011) as well as greater left-hemispheric average minicolumn width. Moreover, there is a greater average distance between mini- (Buxhoeveden et al., 2001; Chance et al., 2006; Economo and Horn, 1930; Seldon, 1981a) and macrocolumns

Table 1
Summary table displaying the results of histological *post mortem* studies on microstructural asymmetry.

Lobe	Area	Brodmann area	Microstructural asymmetry	Citation
Temporal	Planum temporale	BA 22, BA 41, BA 42	Neuron density R > L	Buxhoeveden et al. (2001); Smiley et al. (2011)
Temporal	Planum temporale	BA 22, BA 41, BA 42	Minicolumn width and distance L > R	Seldon (1981a); Buxhoeveden et al. (2001); Economo and Horn (1930); Chance et al. (2006)
Temporal	Planum temporale	BA 22, BA 41, BA 42	Macrocolumn distance L > R	Galuske et al. (2000)
Temporal	Planum temporale	BA 42	Dendritic spread L > R	Seldon (1981a)
Temporal	Planum temporale	BA 22, BA 41, BA 42	Dendritic density L > R	Seldon (1982)
Temporal	Mid-posterior fusiform region	BA 37	Neuron density R > L	Chance et al. (2013)
Temporal	Mid-posterior fusiform region	BA 37	Minicolumn width L > R	Chance et al. (2013)
Temporal	Anterior fusiform cortex	BA 20	Minicolumn width R > L	Di Rosa et al. (2009)
Frontal	Broca's area	BA 44, BA 45	GLI R > L	Amunts et al. (1999); Amunts et al. (2003)
Frontal	Primary motor cortex	BA 4	GLI R > L	Amunts et al. (1996); Amunts et al. (1997)
Frontal	Superior frontal gyrus	BA 9	Neuron density L > R	Cullen et al. (2006)
Frontal	Superior frontal gyrus	BA 9	None	Smiley et al. (2011)
Occipital	V1	BA 17	GLI R > L	Amunts et al. (2007)
Occipital	V2	BA 18	GLI R > L	Amunts et al. (2007)
Occipital	hOc5	–	GLI R > L	Amunts et al. (2007)
Parietal	Supramarginal gyrus	BA 40	Neuron density R > L	Smiley et al. (2012)

(Galuske et al., 2000) in the left hemisphere that is compensated for by greater left-hemispheric dendritic spread (Seldon, 1981a, 1981b) and dendrite density (Seldon, 1982). For the mid-posterior fusiform region (BA 37), greater right-hemispheric neuron density and greater left-hemispheric minicolumn width have been reported (Chance et al., 2013). Greater minicolumn width has also been reported for the right-hemispheric anterior fusiform cortex including BA 20 (Di Rosa et al., 2009). In the frontal lobes, Broca's area (BA 44 and 45) is characterized by a greater GLI in the right hemisphere (Amunts et al., 1999; Amunts et al., 2003). In the primary motor cortex (BA 4), right-hemispheric GLI has been found to be greater than left-hemispheric GLI (Amunts et al., 1996; Amunts et al., 1997). In the superior frontal gyrus (BA 9), greater cell density was found in the left hemisphere (Cullen et al., 2006), while no asymmetry was found in a subsequent study only investigating male brains (Smiley et al., 2011). In the occipital and parietal lobes, analysis of the primary visual cortex (V1, BA 17), V2 (BA 18), and area hOc5, an area sensitive to motion, showed a small interhemispheric asymmetry with lower GLI in the left hemisphere (Amunts et al., 2007). In the inferior parietal lobe, greater neuron density was found in the right supramarginal gyrus (BA 40) (Smiley et al., 2012). One important question is if findings from *post mortem* studies can be replicated *in vivo*. Thus, the second aim of the present study was to compare the results obtained with NODDI with findings from previous histological studies.

2. Materials and methods

2.1. Participants

Asymmetries in gray matter microstructure were investigated in two independent samples from Germany and the US.

German sample. The German sample included 269 participants (143 female) between 18 and 39 years of age (M = 24.35, SD = 4.27). All participants were free from neurodevelopmental, neuropsychiatric, or neurological disorders. Handedness was determined using the Edinburgh handedness inventory (EHI) (Oldfield, 1971). For ten manual actions, participants chose one of five response options (always left, usually left, no preference, usually right, and always right). A lateralization quotient (LQ) was determined by the formula EHI LQ = (R - L)/(R + L) × 100 with L corresponding to the number of left-hand choices and R corresponding to the number of right-hand choices. The corresponding EHI LQ varies between −100 (consistent left-handedness) and +100 (consistent right-handedness). According to Isaacs et al. (2006), participants with an EHI LQ < −60 were classified as left-handed (6.7%, EHI LQ range −100.00 to −62.50, M = −84.75, SD = 13.05), participants with an EHI LQ > −60 and < 60 were classified as ambidextrous (7.8%, EHI LQ range −57.14 to 57.14, M = 23.07, SD = 39.74) and participants with an EHI LQ > 60 were classified as right-handed (85.5%, EHI LQ range 60.00 to 100.00, M = 89.98, SD = 11.64). All participants gave written informed consent and were treated in accordance with the Helsinki declaration. The ethics committee of the Faculty of Psychology at Ruhr University Bochum approved the study procedure.

US sample. The US sample included 251 participants (123 female) between 16 and 39 years of age (M = 22.04, SD = 3.96). Handedness was determined by writing hand, yielding 233 right-handed (92.8%), 12 left-handed (4.8%), and 6 ambidextrous (2.4%) participants. As with the German sample, participants had no history of neurodevelopmental, neuropsychiatric, or neurological disorders and matched the standard inclusion criteria for fMRI examinations. Prior to study enrollment, each participant signed a consent form explaining the procedures and their potential risks. The study and consent form were approved by the University of New Mexico Institutional Review Board.

2.2. Acquisition of imaging data

German sample. Imaging data from the German sample were acquired

using a Philips 3T Achieva scanner equipped with a 32-channel head coil. T1-weighted high-resolution anatomical images were acquired for the purpose of gray and white matter segmentation as well as for the identification of anatomical landmarks (MP-RAGE, TR = 8.18 s, TE = 3.7 ms, flip angle = 8°, 220 sclices, matrix size = 240 × 240, resolution = 1 × 1 × 1 mm). The acquisition time of one individual anatomical image was 6 min. Diffusion-weighted images were acquired using echo planar imaging and the following parameters: TR = 7652 ms, TE = 87 ms, flip angle = 90°, 60 slices, matrix size = 112 × 112, resolution = 2 × 2 × 2 mm. In order to obtain images suitable for NODDI, we employed a multi-shell, high-angular-resolution scheme for which b-values of 1000, 1800, and 2500 s/mm^2 were chosen. Diffusion was measured along 20, 40, and 60 uniformly distributed directions. We utilized the MASSIVE toolbox to ensure that all diffusion directions within and between shells were generated non-colinear to each other. In addition, we obtained eight volumes with no diffusion weighting

(b = 0 s/mm^2) to serve as anatomical reference for motion correction.

US sample. All imaging data from the US sample were acquired at the Mind Research Network in Albuquerque, New Mexico, using a Siemens 3T Trio scanner equipped with a 32-channel head coil. Anatomical images were obtained using an MP-RAGE sequence and the following parameters: TR = 2530 ms, TE = 1.64 ms, flip angle = 7°, 192 slices, matrix size = 256 × 256, resolution = 1 × 1 × 1 mm. Diffusion-weighted images were acquired using echo planar imaging and the following parameters: TR = 3600 ms, TE = 110 ms, flip angle = 84°, 66 slices, matrix size = 96 × 104, resolution = 2.2 × 2.2 × 2.2 mm. In order to obtain images suitable for NODDI, we employed a multi-shell, high-angular-resolution scheme for which b-values of 1000, 2000, and 3000 s/mm^2 were chosen. Diffusion was measured along 24, 48, and 72 uniformly distributed directions. In addition, we obtained six volumes with no diffusion weighting (b = 0 s/mm^2) to serve as anatomical reference for motion correction.
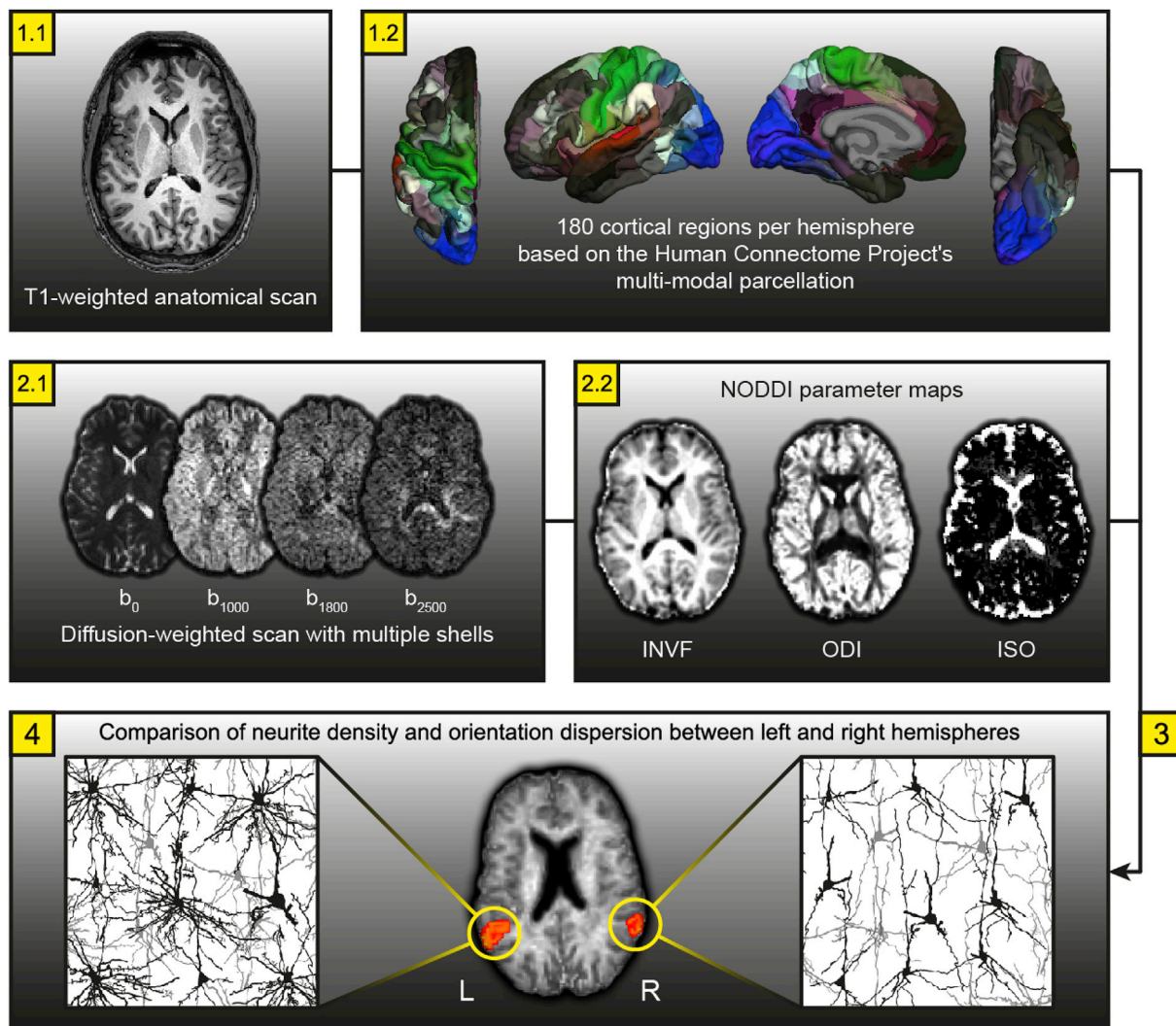
Fig. 1. Schematic overview showing the methodological approach. First, the T1-weighted anatomical scans (1.1) were preprocessed and delineated into 180 cortical areas per hemisphere using the multi-modal parcellation provided by the Human Connectome Project (1.2). Second, the diffusion-weighted scans, each comprising four shells with different b-values (2.1), were preprocessed and analyzed using the AMICO toolbox. This resulted in three NODDI parameter maps of interest (2.2) representing INVF, ODI, and ISO. Third, all cortical brain masks were linearly transformed into the native space of diffusion-weighted scans (3). Fourth, average INVF, ODI, and ISO values were computed for each cortical brain mask and values from the left hemisphere and right hemisphere were compared using a repeated-measures ANCOVA with asymmetry in cortical thickness as a covariate (4). By way of illustration, one slice from an individual INVF map, with left and right PSL regions highlighted in red-to-yellow coloring, is shown in the lower box of this figure. The schematic magnifications next to the INVF map are highly exaggerated depictions showing higher neurite density in the left compared to the right PSL region as found in our data.

2.3. Analysis of imaging data

Surface-based methods in FreeSurfer version 5.3.0 were applied to reconstruct the cortical surface of the T1-weighted images (Dale et al., 1999; Fischl et al., 1999). During preprocessing, skull stripping, gray and white matter segmentation as well as reconstruction and inflation of the cortical surface were performed. Quality control included slice by slice checking for inaccuracies and manual editing if necessary. Automated brain segmentation yielded an estimate of overall cortical volume and overall white matter volume. The Human Connectome Project's multi-modal parcellation (HCPMMP) scheme was applied to delineate the cortex into 180 areas per hemisphere. The HCPMMP has been developed based on the cortical architecture, function, connectivity, and topography from 210 healthy participants (Glasser et al., 2016). After converting the HCPMMP into an annotation file matching fsaverage, FreeSurfer's standard cortical surface, it was further transformed to the individual cortical surface of each participant and converted into volumetric masks. By this procedure, we also obtained individual measures of average cortical thickness for each brain area included in the HCPMMP. Accounting for cortical thickness has been suggested as a method to test whether statistically significant associations observed in NODDI measures in gray matter are influenced by partial volume effects from adjacent white matter (Fukutomi et al., 2018). In order to obtain anatomical landmarks for the extraction of NODDI coefficients, the 360 masks representing the cortical areas of the overall brain were linearly transformed into the native space of the diffusion-weighted images (see Fig. 1).

Preprocessing of diffusion images was performed using FMRIB's Diffusion Toolbox (FDT) in FMRIB Software Library (FSL) version 5.0.7. During preprocessing, eddy current-induced distortions and head movements were simultaneously corrected for using the eddy_correct tool. Gradient directions were corrected to account for nonlinearities. The AMICO toolbox makes use of a convex optimization procedure converting the non-linear fitting into a linear optimization problem (Daducci et al., 2015), which allows for robust estimation of fiber population in considerably reduced processing time (Genç et al., 2018; Sepehrband et al., 2016; Tariq et al., 2016).

The NODDI tissue model distinguishes intra-neurite, extra-neurite and CSF compartments and is based on the fact that water diffusion is affected differently in these environments. First, the intra-cellular compartment represents the space bounded by the membranes of neurites, where water diffusion is highly restricted perpendicular to neurites, but unrestricted along neurites, resulting in symmetric diffusion resembling the shape of sticks or cylinders of zero radius. This intra-neurite volume fraction (INVF) aims to estimate the density of dendrites and axons in gray matter structures and axons in white matter structures. Its underlying model for *in vivo* determination of neurite morphology (Jespersen et al., 2007) has been validated using histological and stereological methods. The diffusion-based estimated neurite density strongly correlates with the intensity of myelin stain under light microscopy (r = 0.91). In contrast, there is a negative correlation with light microscopical staining intensity using Nissl staining (r = −0.56), indicating that the estimated neurite density is negatively related to cell body density. Stereological analysis revealed a strong correlation between estimated neurite density and myelinated axonal density (r = 0.97) indicating that the underlying model mainly reflects myelinated axonal density, with lower values in gray matter compared to white matter (Jespersen et al., 2010). Second, the extra-cellular compartment represents the space outside of neurites, which is characterized by hindered (but not restricted) diffusion. In white matter structures, the extra-cellular compartment is occupied by different types of glia cells, while it is occupied by glia cells and cell bodies in gray matter structures. The orientation dispersion index (ODI) is a tortuosity measure coupling the intra-neurite and the extra-neurite compartment resulting in alignment or dispersion of axons in white matter or axons and dendrites in gray matter. In a validation study, axonal and dendritic orientation distributions were estimated using quantitative analysis of Golgi-stained ferret brain tissue and found to be congruent with respective

MR water diffusion tensors, indicating that the marker for neurite orientation distribution reflects orientation dispersion of both axons and dendrites in gray matter (Jespersen et al., 2012). Third, the cerebrospinal fluid compartment is modeled as isotropic Gaussian diffusion. The isotropic volume fraction (ISO) represents the proportion of free-moving water (Zhang et al., 2012). Recently, NODDI has been validated with human *post mortem* spinal cord tissue. ODI was higher in gray compared to white matter and showed a strong positive correlation with orientation dispersion as quantified by patch-wise circular variance of neurite orientations. In contrast, INVF showed a strong negative correlation with histologically determined neurite orientation dispersion, but a strong positive correlation with myelin staining fraction in gray and white matter (Grussu et al., 2017). Each of the three NODDI coefficients (INVF, ODI, ISO) were computed voxel-wise and averaged for each of the 360 HCPMMP areas.

2.4. Statistical analysis

Hemispheric asymmetries in INVF, ODI, and ISO were analyzed using a repeated-measures ANCOVA for each cortical area with hemisphere (left, right) as within-subject factor and cortical thickness LQ [(cortical thickness right – cortical thickness left)/(cortical thickness lright + cortical thickness left) × 100] of the respective area as covariate. To correct for multiple testing, we used Bonferroni correction for 180 comparisons (α = 0.05/180 = 0.00028). Effect sizes are reported as partial η^2. Analyses were first performed for the German and the US sample individually. A combined effect size for each cortical area was achieved by calculating mean partial η^2 weighted by sample sizes.

Next, we aimed to investigate if microstructural asymmetries are associated with sex or handedness. For INVF, ODI, and ISO, repeated-measures ANCOVAs were conducted for each cortical area with hemisphere (left, right) as within-subject factor, sex as between-subject factor and cortical thickness LQ as covariate. Handedness was analyzed both in terms of handedness category and in terms of continuous hand preference. Left-handed and ambidextrous participants were grouped as non-right-handed due to small group sizes. For handedness category, repeated-measures ANCOVAs were conducted for each cortical area with hemisphere (left, right) as within-subject factor, handedness category (right-handed vs. non-right-handed) as between-subject factor and cortical thickness LQ as covariate. For continuous hand preference, repeated-measures ANCOVAs were calculated with hemisphere (left, right) as within-subject factor and EHI LQ and cortical thickness LQ as covariates. As EHI LQ was only available for the German sample, this analysis was only conducted in this sample. All statistical analysis was performed using SPSS version 20.

While histological studies typically refer to Brodmann areas, we chose a finer subdivision provided by the Human Connectome Project to reveal fine-grained microstructural asymmetries. However, in order to compare the results obtained by NODDI with the results obtained by histological studies, we calculated the overlap between cortical areas that showed asymmetries in either INVF or ODI with Brodmann areas. As there is no histological counterpart for ISO in previous *post mortem* studies on microstructural asymmetries, this analysis was only performed for INVF and ODI. Detailed methods are reported in supplementary material S1.

2.5. Data and code availability statement

Data and code are available from the corresponding author upon reasonable request.

3. Results

3.1. Microstructural asymmetries – consistent effects in both samples

For INVF, the repeated-measures ANCOVAs revealed main effects of hemisphere for 41 cortical areas (22.78% of 180 cortical areas) that were

found in both samples after correction for multiple comparisons (German sample: all $F_{(1,267)} > 14.56$, US sample: all $F_{(1,249)} > 13.69$, all $p < .00028$). Thirteen cortical areas displayed leftward asymmetries in INVF with combined partial η^2 ranging from 0.09 to 0.39. Among these cortical areas were four early auditory areas (STSvp, MI, AVI, FOP5), three frontal areas (10v, p10p, 8Ad), one motor area (FEF), three areas in the inferior parietal cortex (PFop, IP2, PF), and two areas in the temporal-parietal-occipital junction (TPOJ2, PSL) (see Fig. 2). Twenty-eight cortical areas showed rightward asymmetry in INVF in both samples with combined partial η^2 ranging from 0.07 to 0.36. Among these cortical areas were eight in the frontal cortex (p24pr, p32pr, 8BM, a10p, 47l, i6-8, SFL, 46), six in temporal areas (PeEc, TE2p, TE2a, TGv, TGd, TPOJ3), five in sensory and motor areas (3b, 5L, 5m, 24dd, SCEF), four in early and intermediate visual areas (V2, VVC, FFC, VMV3), three in the posterior cortex (LIPv, 7Am, 31pd), and two in early auditory areas (MBelt, 52) (see Fig. 2). Forty-nine cortical areas consistently showed no INVF asymmetry in neither sample. Another 23 cortical areas showed INVF asymmetry towards the same direction, but failed to reach significance after correction for multiple comparisons in one of the two samples (see Table S2).

For ODI, the repeated-measures ANCOVAs revealed main effects of hemisphere for 23 cortical areas (12.78% of 180 cortical areas) in both samples after correction for multiple comparisons (German sample: all $F_{(1,267)} > 13.60$, US sample: all $F_{(1,249)} > 14.00$, all $p < .00028$). Fourteen cortical areas displayed leftward asymmetry in ODI with combined partial η^2 ranging from 0.09 to 0.40. These cortical areas included five areas in the posterior cortex (LIPv, 7Am, IP1, PCV, 23d), four frontal areas (p24pr, 8BM, 13l, SFL), two early auditory areas (A1, MBelt), two motor areas (FOP1, 24dd), and one sensory area (3b) (see Fig. 3). Moreover, nine cortical areas showed significant rightward asymmetries in ODI across both samples with combined partial η^2 ranging from 0.08 to 0.28. Among these areas were five early auditory areas (STSvp, Pol1, Pol2, MI, AVI), two frontal areas (OFC, 8Av), one motor area (6ma), and one early visual area (FFC) (see Fig. 3). Forty-six cortical areas consistently showed no ODI asymmetry in neither sample. Another 22 cortical areas showed ODI asymmetry towards the same direction, but failed to reach significance after correction for multiple comparisons in one of the two samples (see Table S3).

For ISO, the repeated-measures ANCOVAs revealed main effects of hemisphere for 11 cortical areas (6.11% of 180 cortical areas) in both samples after correction for multiple comparisons (German sample: all $F_{(1,267)} > 13.66$, US sample: all $F_{(1,249)} > 13.78$, all $p < .00028$). Four cortical areas showed leftward asymmetry in ISO with combined partial η^2 ranging from 0.05 to 0.10, two in the premotor cortex (6a, 6d), one in

the supplementary motor cortex (6mp), and one in the medial temporal cortex (PreS) (see Fig. 4). Seven cortical areas showed significant rightward asymmetry in both samples with combined partial η^2 ranging from 0.06 to 0.31. Among these areas, two were in frontal areas (IFSa, OFC), two were in medial and lateral temporal areas (TGv, PeEc), one in the auditory cortex (STSva), one in the visual cortex (VVC) and one in the somatosensory cortex (3a) (see Fig. 4). Among the 180 cortical areas, 101 consistently showed no ISO asymmetry in neither sample. Another 16 cortical areas showed ISO asymmetry towards the same direction, but failed to reach significance after correction for multiple comparisons in one of the two samples (see Table S4).

The overlap of cortical areas showing asymmetries in INVF or ODI with Brodmann areas is reported in supplementary material S1.

3.2. Microstructural asymmetries – opposite effects in both samples

For INVF, 45 cortical areas showed a significant asymmetry in one of the samples, but not the other (see Table S5). Thirteen cortical areas showed asymmetries in opposite directions, but only survived correction for multiple comparisons in one of the samples. Moreover, eight cortical areas showed significant INVF asymmetry in both samples, but with opposite directions. This applied to somatosensory (3a), temporal (A4, A5, EC, PI), parietal (IP0), premotor (PEF) and visual cortical areas (V3B).

For ODI, 51 cortical areas showed significant asymmetry in one sample, but not in the other (see Table S6). Twenty-one cortical areas showed asymmetries in opposite directions, but only survived correction for multiple comparisons in one of the samples. Seventeen cortical areas displayed significant opposite effects in the samples. These areas were concentrated in visual (V8, V4t, V3B), auditory (STSdp, STSda, Pir, FOP4, 52), parietal (PFm, 7 PC, 31pv), and frontal areas (p24, 9m, 10d, 55b) as well as in the temporal-parietal junction (PSL, TPOJ2).

Forty-one cortical areas showed significant ISO asymmetry in one, but not the other sample (see Table S7). Nine cortical areas showed asymmetries in opposite directions, but only survived correction for multiple comparisons in one of the samples. Two cortical areas in the lateral temporal cortex (TF) and the early visual cortex (V2) displayed significant opposite effects.

3.3. Effects of handedness

For handedness category, repeated-measures ANCOVAs revealed no significant hemisphere by handedness interaction in neither the German
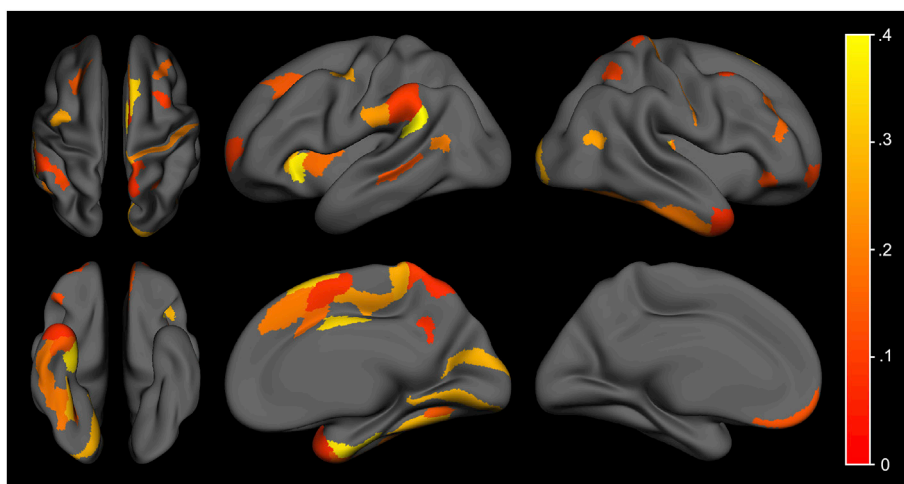
Fig. 2. Consistent microstructural asymmetries in INVF over both samples. The color scale represents the effect size of the main effect of hemisphere from small (red) to large (yellow). Microstructural asymmetries on the brain surface are shown from above, from a lateral view (left and right), from below, and from a medial view (right and left), respectively.
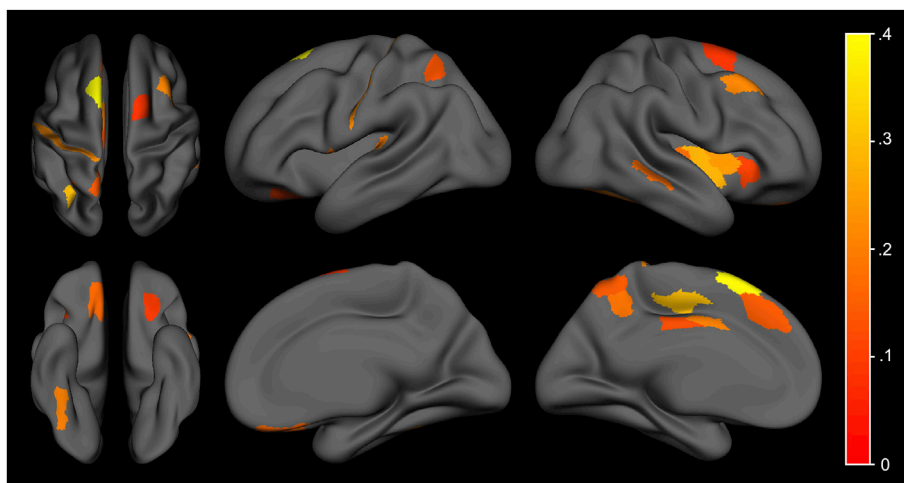
Fig. 3. Consistent microstructural asymmetries in ODI over both samples. The color scale represents the effect size of the main effect of hemisphere from small (red) to large (yellow). Microstructural asymmetries on the brain surface are shown from above, from a lateral view (left and right), from below, and from a medial view (right and left), respectively.
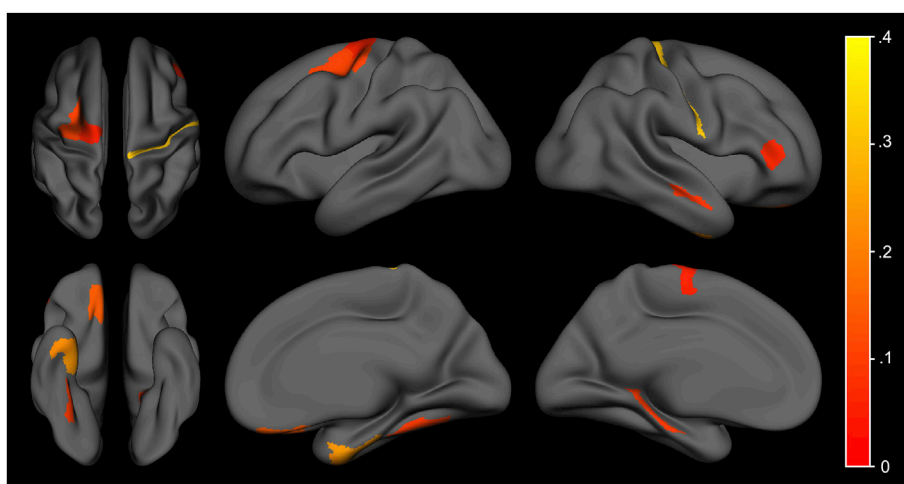

Fig. 4. Consistent microstructural asymmetries in ISO over both samples. The color scale represents the effect size of the main effect of hemisphere from small (red) to large (yellow). Microstructural asymmetries on the brain surface are shown from above, from a lateral view (left and right), from below, and from a medial view (right and left), respectively.

nor the US sample for INVF (German sample: all $F_{(1,266)} < 9.70$, all $p > .00028$, all partial $\eta^2 < 0.04$; US sample: all $F_{(1,248)} < 8.50$, all $p > .00028$, all partial $\eta^2 < 0.04$), ODI (German sample: all $F_{(1,266)} < 7.22$, all $p > .00028$, all partial $\eta^2 < 0.03$; US sample: all $F_{(1,248)} < 7.53$, all $p > .00028$, all partial $\eta^2 < 0.03$), and ISO (German sample: all $F_{(1,266)} < 11.06$, all $p > .00028$, all partial $\eta^2 < 0.04$; US sample: all $F_{(1,248)} < 5.79$, all $p > .00028$, all partial $\eta^2 < 0.03$).

For continuous hand preference, which was only available for the German sample, repeated-measures ANCOVAs revealed no significant hemisphere by EHI LQ interactions for ODI (all $F_{(1,266)} < 9.15$, all $p > .00028$, all partial $\eta^2 < 0.03$) or ISO (all $F_{(1,266)} < 13.45$, all $p > .00028$, all partial $\eta^2 < 0.05$). There was a significant hemisphere by EHI LQ interaction for INVF in cortical area TPOJ3 ($F_{(1,266)} = 15.66$, $p < .00028$, partial $\eta^2 = 0.06$).

3.4. Effects of sex

Repeated-measures ANCOVAs revealed no hemisphere by sex interactions for INVF in neither the German sample (all $F_{(1,266)} < 10.10$, all $p > .00028$, all partial $\eta^2 < 0.04$) or the US sample (all $F_{(1,248)} < 11.83$, all $p > .00028$, all partial $\eta^2 < 0.05$) after correction for multiple comparisons. For ODI, there was a significant hemisphere by sex interaction for cortical area V3A in the German sample ($F_{(1,266)} = 15.60$, $p < .00028$, partial $\eta^2 = 0.06$) and for cortical area 5m in the US sample ($F_{(1,248)} = 22.18$, $p < .00028$, partial $\eta^2 = 0.08$). However, no cortical area showed a significant hemisphere by sex interaction in both samples. There were no significant interactions for ISO in neither sample (German sample: all $F_{(1,266)} < 11.20$, all $p > .00028$, all partial $\eta^2 < 0.04$; US sample: all $F_{(1,248)} < 7.20$, all $p > .00028$, all partial $\eta^2 < 0.03$).

4. Discussion

Hemispheric asymmetries in microstructure have mainly been investigated in histological *post mortem* studies, which are usually characterized by small samples, clearly defined cortical areas and non-conservative exclusion criteria (e.g. regarding neurological causes of death). NODDI aims to estimate neurite density and its orientation distribution *in vivo* (Zhang et al., 2012), thereby providing the opportunity to investigate microstructural asymmetries in large samples and across the whole brain. This is crucially important for laterality research to enable the investigation of structure-function relationships on the microstructural level. Studies attempting to predict handedness

(Guadalupe et al., 2014; Ocklenburg et al., 2016b) or language laterali-zation (Greve et al., 2013) by gray matter macrostructure reported low correlations of structure and function. Thus, as suggested by Ocklenburg et al. (2016a), macrostructural studies should be complemented by microstructural studies. Recently, the first hint towards a functional impact of microstructural asymmetries indicated by NODDI has been reported. Greater INVF in the left *planum temporale* has been associated with the latency of the N1 ERP component in the left hemisphere during a passive dichotic listening paradigm, suggesting that greater left- than right-hemispheric INVF in the posterior temporal lobe reflects faster left-hemispheric neurophysiological processing of language (Ocklenburg et al., 2018).

Here, NODDI revealed substantial microstructural asymmetries as 22.78% of cortical areas showed asymmetrical INVF. Leftward asym-metries were concentrated in early auditory and orbitofrontal areas, while rightward asymmetries were mainly found in early and interme-diate visual areas, the inferior temporal lobe and sensory-motor areas. Overall, 12.78% of cortical areas showed asymmetrical ODI with left-ward asymmetry mainly found in frontal and medial parietal areas. Rightward asymmetry in ODI was concentrated in early auditory and motor areas. Moreover, 6.11% of cortical areas showed asymmetrical ISO across both samples. As these areas show microstructural asymmetries towards the same direction in two independent datasets, it is assumed that microstructural asymmetries in these cortical areas are highly reli-able. Employing multiple large datasets for the purpose of study repli-cation has been suggested as one way to successfully address the replication crisis in neuroscience (Kellmeyer, 2017). Overall, there were hardly any effects of neither sex nor handedness on asymmetry of NODDI parameters.

4.1. Accordance with post mortem studies

Histological studies found greater neuron density in the right *planum temporale* (Buxhoeveden et al., 2001; Smiley et al., 2011) and inferior parietal lobe (Smiley et al., 2012). In line with these findings, our results show greater left-than right-hemispheric INVF in the auditory association cortex and temporo-parietal occipital junction, with strongest leftward asymmetry in cortical area PSL (perisylvian language area) (see Fig. 2). This is also in line with the finding of greater left-hemispheric dendrite density (Seldon, 1982). Moreover, assuming that greater distance be-tween minicolumns reflects higher neuropil density (Seldon, 1981a), our findings are in line with studies reporting wider and more distant left-hemispheric mini- (Buxhoeveden et al., 2001; Chance et al., 2006; Economo and Horn, 1930; Seldon, 1981a) and macrocolumns (Galuske et al., 2000). Greater dendritic spread in the left hemisphere (Seldon, 1981a) is in accordance with ODI being left-lateralized in early auditory regions (see Fig. 3). Overall, NODDI parameters successfully reflect what has been found in histological *post mortem* studies in the temporal and inferior parietal lobe.

Greater cell body density in the left superior frontal gyrus (Cullen et al., 2006) is reflected by higher right-hemispheric INVF in the central dorsolateral and medial superior prefrontal cortex. In contrast, the dorsal middle frontal gyrus shows greater left- than right-hemispheric INVF. Thus, the contrasting finding of microstructural symmetry in the superior frontal gyrus (Smiley et al., 2011) might be due to structural differences within BA 9 that become evident in finer subdivisions. Greater mini-column width has been reported in the left fusiform gyrus (Chance et al., 2013). Thus, it has been suggested that wide minicolumns foster fine discrimination while narrow minicolumns are beneficial for holistic processing (Chance, 2014). However, our data indicate that INVF is greater in the right hemisphere dominant for face processing. This is in line with the finding of wider minicolumn spacing in the right-hemispheric fusiform gyrus (Di Rosa et al., 2009).

For Broca's area (BA 44 and 45), higher cell body density has been reported for the right hemisphere (Amunts et al., 2003). In contrast, our data do not show microstructural asymmetries in either INVF, ODI, or

ISO in Broca's area. However, the sample reported by Amunts et al. (2003) is an extended sample from an initial small sample of n = 10 (37–85 years). In the initial sample, left-hemispheric asymmetry in cell body density was found for BA 44, but not BA 45 (Amunts et al., 1999). The extended sample of n = 34 (3.5 months - 85 years), including the initial sample, showed a right-hemispheric asymmetry, but only when the two areas were condensed (Amunts et al., 2003; Schenker et al., 2009). It might be that subtle asymmetries in small cortical areas accu-mulate when analyzing them together. However, Hutsler and Galuske (2003) refer to unpublished data indicating an absence of asymmetry in macrocolumn width or distance in Broca's area. On a fine-grained level, we found no asymmetries regarding microstructure in Broca's area as determined by NODDI. This is consistent with the conclusion that the functional asymmetry of Broca's area is not equivalent to an underlying consistent structural asymmetry (Keller et al., 2009). For the primary motor cortex, greater right- than left-hemispheric cell body density has been reported in histological studies, suggesting less neuropil in the right region of hand representation (Amunts et al., 1996, 1997). This region is broadly represented by HCPMMP area 4 (primary motor cortex) which is symmetrical in INVF, ODI, and ISO in our samples.

4.2. Beyond post mortem studies

NODDI allows for the investigation of microstructural asymmetries across the whole brain, enabling not only a replication of previous studies, but revealing asymmetries beyond what has been reported in histological studies. We found greater left- than right-hemispheric INVF in the insular and frontal opercular cortex [MI (middle insular area), AVI (anterior ventral insular area), FOP5 (frontal opercular area 5)]. The effect of INVF in AVI being left-lateralized was one of the strongest effects seen over both samples (see Fig. 2). Interestingly, volume asymmetry of the insula is associated with language lateralization (Keller et al., 2011) and functional activity during gesturing (Biduła and Króliczak, 2015), suggesting that insular macrostructural asymmetry has a functional relevance for hemispheric asymmetries. Future studies will elucidate if microstructural asymmetry has similar potential for functional laterali-zation. Moreover, we found right-greater-than-left INVF in the superior parietal cortex [LIPv (lateral intraparietal ventral area), 7Am (medial subdivision of area 7A)] and interspersed over the frontal cortex [p24r (proisocortex), p32pr (paralimbic region), 8BM, a10p, 47l, i6-8 (inferior transitional area between BA 6 and BA 8), SFL (superior frontal language area)].

ODI showed leftward asymmetry in the superior parietal cortex [LIPv (lateral intraparietal ventral area), 7Am (medial subdivision of area 7A)] and parts of the frontal cortex [p24r (proisocortex), 13l, 8BM, SFL (su-perior frontal language area)]. This INVF leftward asymmetry of SFL was the strongest asymmetry in ODI seen over both samples (see Fig. 3). Functional imaging has established the superior frontal gyrus as part of a cluster showing leftward activation during the dichotic listening task, a common task determining language lateralization (Westerhausen et al., 2014). Future research should determine the association of ODI asym-metry in SFL with language lateralization. Moreover, ODI was greater in the right insular and frontal opercular cortex [Pol1 and Pol2 (posterior insular area 1 and 2), MI (middle insular area), AVI (anterior ventral insular area)], which is also interesting in the context of macrostructural insular asymmetries (Biduła and Króliczak, 2015; Keller et al., 2011).

4.3. Limitations and outlook

In this work, we specifically investigated gray matter microstructural asymmetries as determined by NODDI. While our results are in line with what has been reported in histological studies, it is important to emphasize that it remains unclear to what extent NODDI parameters reflect microstructural features as determined in *post mortem* tissue, especially in gray matter. In rats, it has been shown that diffusion-based estimated neurite density reflects myelinated axonal density, with higher

values in white matter as compared to gray matter (Jespersen et al., 2010). In ferret brain tissue, ODI shows a positive association with orientation distribution from Golgi-staining, which visualizes neurites and somata in gray matter (Jespersen et al., 2012). A validation study in human spinal cord supported these findings and showed higher ODI values in gray compared to white matter (Grussu et al., 2017). However, the findings obtained in the current study should not be interpreted as a definite representation of microstructural features determined in histological studies. Especially the relation of NODDI with very specific features such as mini- and macrocolumn distance remains speculative. In addition to this general limitation of NODDI, its application is by far less precise than what is possible in *post mortem* studies. First, INVF, ODI, and ISO represent only a fraction of markers for microstructural asymmetry that can be investigated in histological studies. Second, *in vivo* MRI is not suited for comparing proximal and distal dendritic segments (Scheibel et al., 1985) or layer-specific analyses (Hayes and Lewis, 1996), which would require a higher resolution than what is possible using 3T.

Despite these limitations, NODDI offers new opportunities in the context of clinical applications. Recently, NODDI was applied to individuals with schizophrenia and healthy controls. The authors found lower bilateral INVF in the rostromedial temporal lobe and higher ODI in the left posterior cingulate, supplementary motor, and lateral occipital cortex in individuals with schizophrenia (Nazeri et al., 2017). Future studies should determine if these findings are in line with atypical microstructural asymmetry in schizophrenia (Chance et al., 2008; Chance, 2014; Cullen et al., 2006; Simper et al., 2011). A reversal of microstructural asymmetry has also been reported for other neuropathological conditions such as Alzheimer's disease (Kutová et al., 2014) and would be worthwhile to investigate using NODDI.

4.4. Conclusion

Taken together, this is the first *in vivo* study to determine microstructural gray matter asymmetries in INVF, ODI, and ISO in a large dataset of 520 healthy individuals. NODDI not only reflects findings from histological studies, but also reveals microstructural asymmetries beyond *post mortem* findings, suggesting to investigate asymmetries in the insular, frontal opercular, and superior parietal cortex. Future studies will reveal if asymmetries in microstructure reflect functional hemispheric dominance for specific cognitive domains.

Acknowledgements

Appendix A. Supplementary data

Supplementary data to this article can be found online at https://doi.org/10.1016/j.neuroimage.2019.01.079.

References

Amunts, K., Schlaug, G., Schleicher, A., Steinmetz, H., Dabringhaus, A., Roland, P.E., Zilles, K., 1996. Asymmetry in the human motor cortex and handedness. Neuroimage 4 (3 Pt 1), 216–222. https://doi.org/10.1006/nimg.1996.0073.

Amunts, K., Schleicher, A., Bürgel, U., Mohlberg, H., Uylings, H.B., Zilles, K., 1999. Broca's region revisited: Cytoarchitecture and intersubject variability. J. Comp. Neurol. 412 (2), 319–341.

Amunts, K., Schmidt-Passos, F., Schleicher, A., Zilles, K., 1997. Postnatal development of interhemispheric asymmetry in the cytoarchitecture of human area 4. Anat. Embryol. 196 (5), 393–402.

Amunts, K., Armstrong, E., Malikovic, A., Hömke, L., Mohlberg, H., Schleicher, A., Zilles, K., 2007. Gender-specific left-right asymmetries in human visual cortex. J. Neurosci. : Offic. J. Soc. Neurosci. 27 (6), 1356–1364. https://doi.org/10.1523/JNEUROSCI.4753-06.2007.

Amunts, K., Schleicher, A., Ditterich, A., Zilles, K., 2003. Broca's region: Cytoarchitectonic asymmetry and developmental changes. J. Comp. Neurol. 465 (1), 72–89. https://doi.org/10.1002/cne.10829.

Armour, J.A.L., Davison, A., McManus, I.C., 2014. Genome-wide association study of handedness excludes simple genetic models. Heredity 112 (3), 221–225. https://doi.org/10.1038/hdy.2013.93.

Biduła, S.P., Króliczak, G., 2015. Structural asymmetry of the insula is linked to the lateralization of gesture and language. Eur. J. Neurosci. 41 (11), 1438–1447. https://doi.org/10.1111/ejn.12888.

Brandler, W.M., Morris, A.P., Evans, D.M., Scerri, T.S., Kemp, J.P., Timpson, N.J., et al., 2013. Common variants in left/right asymmetry genes and pathways are associated with relative hand skill. PLoS Genet. 9 (9), e1003751. https://doi.org/10.1371/journal.pgen.1003751.

Buxhoeveden, D.P., Switala, A.E., Litaker, M., Roy, E., Casanova, M.F., 2001. Lateralization of minicolumns in human planum temporale is absent in nonhuman primate cortex. Brain Behav. Evol. 57 (6), 349–358.

Casanova, M.F., van Kooten, I.A.J., Switala, A.E., van Engeland, H., Heinsen, H., Steinbusch, H.W.M., et al., 2006. Minicolumnar abnormalities in autism. Acta Neuropathol. 112 (3), 287–303. https://doi.org/10.1007/s00401-006-0085-5.

Chance, S.A., Casanova, M.F., Switala, A.E., Crow, T.J., 2006. Minicolumnar structure in Heschl's gyrus and planum temporale: Asymmetries in relation to sex and callosal fiber number. Neuroscience 143 (4), 1041–1050. https://doi.org/10.1016/j.neuroscience.2006.08.057.

Chance, S.A., 2014. The cortical microstructural basis of lateralized cognition: A review. Front. Psychol. 5, 820. https://doi.org/10.3389/fpsyg.2014.00820.

Chance, S.A., Casanova, M.F., Switala, A.E., Crow, T.J., 2008. Auditory cortex asymmetry, altered minicolumn spacing and absence of ageing effects in schizophrenia. Brain : J. Neurol. 131 (Pt 12), 3178–3192. https://doi.org/10.1093/brain/awn211.

Chance, S.A., Sawyer, E.K., Clover, L.M., Wicinski, B., Hof, P.R., Crow, T.J., 2013. Hemispheric asymmetry in the fusiform gyrus distinguishes Homo sapiens from chimpanzees. Brain Struct. Funct. 218 (6), 1391–1405. https://doi.org/10.1007/s00429-012-0464-8.

Cullen, T.J., Walker, M.A., Eastwood, S.L., Esiri, M.M., Harrison, P.J., Crow, T.J., 2006. Anomalies of asymmetry of pyramidal cell density and structure in dorsolateral prefrontal cortex in schizophrenia. Br. J. Psychiatry : J. Ment. Sci. 188, 26–31. https://doi.org/10.1192/bjp.bp.104.008169.

Daducci, A., Canales-Rodríguez, E.J., Zhang, H., Dyrby, T.B., Alexander, D.C., Thiran, J.-P., 2015. Accelerated Microstructure Imaging via Convex Optimization (AMICO) from diffusion MRI data. Neuroimage 105, 32–44. https://doi.org/10.1016/j.neuroimage.2014.10.026.

Dale, A.M., Fischl, B., Sereno, M.I., 1999. Cortical surface-based analysis. I. Segmentation and surface reconstruction. Neuroimage 9 (2), 179–194. https://doi.org/10.1006/nimg.1998.0395.

Di Rosa, E., Crow, T.J., Walker, M.A., Black, G., Chance, S.A., 2009. Reduced neuron density, enlarged minicolumn spacing and altered ageing effects in fusiform cortex in schizophrenia. Psychiatr. Res. 166 (2–3), 102–115. https://doi.org/10.1016/j.psychres.2008.04.007.

Economo, C. von, Horn, L., 1930. Über Windungsrelief, Maße und Rindenarchitektonik der Supratemporalfläche, ihre individuellen und ihre Seitenunterschiede. Zeitschrift für die gesamte Neurologie und Psychiatrie 130 (1), 678–757. https://doi.org/10.1007/BF02865945.

Fischl, B., Sereno, M.I., Dale, A.M., 1999. Cortical surface-based analysis. II: Inflation, flattening, and a surface-based coordinate system. Neuroimage 9 (2), 195–207. https://doi.org/10.1006/nimg.1998.0396.

Fukutomi, H., Glasser, M.F., Zhang, H., Autio, J.A., Coalson, T.S., Okada, T., et al., 2018. Neurite imaging reveals microstructural variations in human cerebral cortical gray matter. Neuroimage 182, 488–499. https://doi.org/10.1016/j.neuroimage.2018.02.017.

Galuske, R.A., Schlote, W., Bratzke, H., Singer, W., 2000. Interhemispheric asymmetries of the modular structure in human temporal cortex. Science (New York, N.Y.) 289 (5486), 1946–1949.

Genç, E., Fraenz, C., Schlüter, C., Friedrich, P., Hossiep, R., Voelkle, M.C., et al., 2018. Diffusion markers of dendritic density and arborization in gray matter predict differences in intelligence. Nat. Commun. 9 (1), 1905. https://doi.org/10.1038/s41467-018-04268-8.

Glasser, M.F., Coalson, T.S., Robinson, E.C., Hacker, C.D., Harwell, J., Yacoub, E., et al., 2016. A multi-modal parcellation of human cerebral cortex. Nature 536 (7615), 171–178. https://doi.org/10.1038/nature18933.

Greve, D.N., van der Haegen, L., Cai, Q., Stufflebeam, S., Sabuncu, M.R., Fischl, B., Brysbaert, M., 2013. A surface-based analysis of language lateralization and cortical asymmetry. J. Cognit. Neurosci. 25 (9), 1477–1492. https://doi.org/10.1162/jocn_a_00405.

Grussu, F., Schneider, T., Tur, C., Yates, R.L., Tachrount, M., Ianuş, A., et al., 2017. Neurite dispersion: a new marker of multiple sclerosis spinal cord pathology? Ann. Clin. Transl. Neurol. 4 (9), 663–679. https://doi.org/10.1002/acn3.445.

Guadalupe, T., Willems, R.M., Zwiers, M.P., Arias Vasquez, A., Hoogman, M., Hagoort, P., et al., 2014. Differences in cerebral cortical anatomy of left- and right-handers. Front. Psychol. 5, 261. https://doi.org/10.3389/fpsyg.2014.00261.

Güntürkün, O., Ocklenburg, S., 2017. Ontogenesis of Lateralization. Neuron 94 (2), 249–263. https://doi.org/10.1016/j.neuron.2017.02.045.

Hayes, T.L., Lewis, D.A., 1996. Magnopyramidal neurons in the anterior motor speech region. Dendritic features and interhemispheric comparisons. Arch. Neurol. 53 (12), 1277–1283.

Hutsler, J., Galuske, R.A.W., 2003. Hemispheric asymmetries in cerebral cortical networks. Trends Neurosci. 26 (8), 429–435. https://doi.org/10.1016/S0166-2236(03)00198-X.

Isaacs, K.L., Barr, W.B., Nelson, P.K., Devinsky, O., 2006. Degree of handedness and cerebral dominance. Neurology 66 (12), 1855–1858. https://doi.org/10.1212/01.wnl.0000219623.28769.74.

Jespersen, S.N., Bjarkam, C.R., Nyengaard, J.R., Chakravarty, M.M., Hansen, B., Vosegaard, T., et al., 2010. Neurite density from magnetic resonance diffusion measurements at ultrahigh field: Comparison with light microscopy and electron microscopy. Neuroimage 49 (1), 205–216. https://doi.org/10.1016/j.neuroimage.2009.08.053.

Jespersen, S.N., Kroenke, C.D., Østergaard, L., Ackerman, J.J.H., Yablonskiy, D.A., 2007. Modeling dendrite density from magnetic resonance diffusion measurements. Neuroimage 34 (4), 1473–1486. https://doi.org/10.1016/j.neuroimage.2006.10.037.

Jespersen, S.N., Leigland, L.A., Cornea, A., Kroenke, C.D., 2012. Determination of axonal and dendritic orientation distributions within the developing cerebral cortex by diffusion tensor imaging. IEEE Trans. Med. Imag. 31 (1), 16–32. https://doi.org/10.1109/TMI.2011.2162099.

Keller, S.S., Crow, T., Foundas, A., Amunts, K., Roberts, N., 2009. Broca's area: nomenclature, anatomy, typology and asymmetry. Brain Lang. 109 (1), 29–48. https://doi.org/10.1016/j.bandl.2008.11.005.

Keller, S.S., Roberts, N., García-Fiñana, M., Mohammadi, S., Ringelstein, E.B., Knecht, S., Deppe, M., 2011. Can the language-dominant hemisphere be predicted by brain anatomy? J. Cognit. Neurosci. 23 (8), 2013–2029. https://doi.org/10.1162/jocn.2010.21563.

Kellmeyer, P., 2017. Ethical and Legal Implications of the Methodological Crisis in Neuroimaging. Camb. Q. Healthc. Ethics : CQ : Int. J. Healthc. Ethics Committees 26 (4), 530–554. https://doi.org/10.1017/S096318011700007X.

Kutová, M., Mrzílková, J., Kirdajová, D., Řípová, D., Zach, P., 2014. Simple method for evaluation of planum temporale pyramidal neurons shrinkage in postmortem tissue of Alzheimer disease patients. BioMed Res. Int. 2014, 607171. https://doi.org/10.1155/2014/607171.

Nazeri, A., Mulsant, B.H., Rajji, T.K., Levesque, M.L., Pipitone, J., Stefanik, L., Shahab, S., Roostaei, T., Wheeler, A.L., Chavez, S., Voineskos, A.N., 2017. Gray matter neuritic microstructure deficits in schizophrenia and bipolar disorder. Biol. Psychiatry. 82 (10), 726–736. https://doi.org/10.1016/j.biopsych.2016.12.005.

Ocklenburg, S., Beste, C., Arning, L., Peterburs, J., Güntürkün, O., 2014. The ontogenesis of language lateralization and its relation to handedness. Neurosci. Biobehav. Rev. 43, 191–198. https://doi.org/10.1016/j.neubiorev.2014.04.008.

Ocklenburg, S., Friedrich, P., Fraenz, C., Schlüter, C., Beste, C., Güntürkün, O., Genç, E., 2018. Neurite architecture of the planum temporale predicts neurophysiological processing of auditory speech. Sci. Adv. 4 (7), eaar6830. https://doi.org/10.1126/sciadv.aar6830.

Ocklenburg, S., Friedrich, P., Güntürkün, O., Genç, E., 2016a. Intrahemispheric white matter asymmetries: The missing link between brain structure and functional lateralization? Rev. Neurosci. 27 (5), 465–480. https://doi.org/10.1515/revneuro-2015-0052.

Ocklenburg, S., Friedrich, P., Güntürkün, O., Genç, E., 2016b. Voxel-wise grey matter asymmetry analysis in left- and right-handers. Neurosci. Lett. 633, 210–214. https://doi.org/10.1016/j.neulet.2016.09.046.

Ocklenburg, S., Güntürkün, O., 2018. The lateralized brain: The neuroscience and evolution of hemispheric asymmetries. Academic Press, London.

Oldfield, R.C., 1971. The assessment and analysis of handedness: The Edinburgh inventory. Neuropsychologia 9 (1), 97–113.

Scheibel, A.B., Paul, L.A., Fried, I., Forsythe, A.B., Tomiyasu, U., Wechsler, A., et al., 1985. Dendritic organization of the anterior speech area. Exp. Neurol. 87 (1), 109–117.

Schenker, N.M., Sherwood, C.C., Hof, P.R., Semendeferi, K., 2009. Microstructural Asymmetries of the Cerebral Cortex in Humans and Other Mammals. In: Hopkins, W.D. (Ed.), Special Topics in Primatology. The Evolution of hemispheric specialization in primates, vol. 5. Academic Press; American Society of Primatologists, London, Norman, Oklahoma, pp. 92–118. https://doi.org/10.1016/S1936-8526(07)05004-X.

Schmitz, J., Metz, G.A.S., Güntürkün, O., Ocklenburg, S., 2017. Beyond the genome-Towards an epigenetic understanding of handedness ontogenesis. Prog. Neurobiol. 159, 69–89. https://doi.org/10.1016/j.pneurobio.2017.10.005.

Seldon, H.L., 1981a. Structure of human auditory cortex. I. Cytoarchitectonics and dendritic distributions. Brain Res. 229 (2), 277–294.

Seldon, H.L., 1981b. Structure of human auditory cortex. II. Axon distributions and morphological correlates of speech perception. Brain Res. 229 (2), 295–310.

Seldon, H.L., 1982. Structure of human auditory cortex. III. Statistical analysis of dendritic trees. Brain Res. 249 (2), 211–221.

Sepehrband, F., Alexander, D.C., Kurniawan, N.D., Reutens, D.C., Yang, Z., 2016. Towards higher sensitivity and stability of axon diameter estimation with diffusion-weighted MRI. NMR Biomed. 29 (3), 293–308. https://doi.org/10.1002/nbm.3462.

Simper, R., Walker, M.A., Black, G., Di Rosa, E., Crow, T.J., Chance, S.A., 2011. The relationship between callosal axons and cortical neurons in the planum temporale: Alterations in schizophrenia. Neurosci. Res. 71 (4), 405–410. https://doi.org/10.1016/j.neures.2011.08.007.

Smiley, J.F., Konnova, K., Bleiwas, C., 2012. Cortical thickness, neuron density and size in the inferior parietal lobe in schizophrenia. Schizophr. Res. 136 (1–3), 43–50. https://doi.org/10.1016/j.schres.2012.01.006.

Smiley, J.F., Rosoklija, G., Mancevski, B., Pergolizzi, D., Figarsky, K., Bleiwas, C., et al., 2011. Hemispheric comparisons of neuron density in the planum temporale of schizophrenia and nonpsychiatric brains. Psychiatr. Res. 192 (1), 1–11. https://doi.org/10.1016/j.pscychresns.2010.11.007.

Tariq, M., Schneider, T., Alexander, D.C., Gandini Wheeler-Kingshott, C.A., Zhang, H., 2016. Bingham-NODDI: Mapping anisotropic orientation dispersion of neurites using diffusion MRI. Neuroimage 133, 207–223. https://doi.org/10.1016/j.neuroimage.2016.01.046.

van Kooten, I.A.J., Palmen, S.J.M.C., Cappeln, P. von, Steinbusch, H.W.M., Korr, H., Heinsen, H., et al., 2008. Neurons in the fusiform gyrus are fewer and smaller in autism. Brain : J. Neurol. 131 (Pt 4), 987–999. https://doi.org/10.1093/brain/awn033.

Westerhausen, R., Kompus, K., Hugdahl, K., 2014. Mapping hemispheric symmetries, relative asymmetries, and absolute asymmetries underlying the auditory laterality effect. Neuroimage 84, 962–970. https://doi.org/10.1016/j.neuroimage.2013.09.074.

Zhang, H., Schneider, T., Wheeler-Kingshott, C.A., Alexander, D.C., 2012. NODDI: Practical in vivo neurite orientation dispersion and density imaging of the human brain. Neuroimage 61 (4), 1000–1016. https://doi.org/10.1016/j.neuroimage.2012.03.072.